where ρ_f is the specific density of the fuel, which is 0.84 for gas oil. The SFC, which shows its minimum value at an equivalence ratio higher than 0.6, increases with decreasing equivalence ratio, and reaches infinity at an equivalence ratio satisfying the following condition:

$$Q_i = Q_{mL} + Q_{gL}, \qquad Q_{kW} = 0. \tag{33}$$

For decreasing the SFC of a diesel-electric generator plant, it is most important to select a diesel engine having a small mechanical loss Q_{mL} and an electric generator having a small generator loss Q_{gL} and, moreover, to select a normal running state to correspond to the equivalence ratio giving a minimum SFC.

The yearly mean SFC of the 110-kVA diesel-electric generator plant observed in JARE-20 was only 0.328 l/kWh, and the power plant efficiency was 28.8%, but the greater part of the waste heat of the engine was recovered and used for making cold water by melting ice or snow, and for heating hot water for room-heating and bathtub uses at both Syowa and Mizuho Stations in Antarctica.

6. Exhaust-Gas Heat Exchangers

Several types of exhaust gas to water heat exchangers as described below were developed by the authors.

6.1. Shell-and-coil type exhaust-gas heat exchangers

During about twenty years from JARE-1 to JARE-18 (1956/76), the shell-and-coil heat exchangers were used for recovering the waste heat from exhaust gas of diesel engines coupled to electric generators. Their main design data are shown in Table 7 and their features are shown in Figs. 2, 5, 6, 29, 30 and 31. The heat exchanger is composed of a cylindrical stainless shell, a top cover plate with water inlet and outlet headers connected to three or four coils, and a center duct. The hot exhaust gas of a diesel engine flows tangentially into the shell at a point near the top end thereof and swirls downward around the coils. When it reaches the bottom end of the shell, it turns up through the center duct to a chimney. On the one hand, cold water pressurized by a pump is led to the inlet header on the top cover plate and is divided and fed to each coil. While the water is flowing through the coil tubes, it absorbs the waste exhaust-gas energy and is led to an outlet header on the top cover plate. The heat exchangers used were very compact and effective and could absorb about 60% of the waste exhaust-gas energy as shown in Table A-4 in Appendix, but some difficulties were experienced as described below.

(*a*) *Acid corrosion of coils*

When the heat exchanger was used for heating cold water of the ice-melting tank directly, the outlet gas temperature was occasionally decreased to about 50–55°C, and the combustion gas contacted very cold coil surfaces, so that some of the water vapor contained in the combustion gas condensed on the coil surfaces. The gas-oil fuel contains about 0.4% sulphur, and its combustion gas contains about 0.025% of SO_2, about 3% of which changes to SO_3. The SO_3 component combines with the condensed water to form H_2SO_4. The corrosion effect of H_2SO_4 on stainless steel is very significant. It causes severe pitting corrosion

Table 7. Shell-and-coil type exhaust-gas heat exchanger for JARE.

Items	JARE-1 (1956/58)	JARE-2 (1957/59)	JARE-7/15 (1965/75)	JARE-16/18 (1974/78)	Remarks
Capacity (kcal/h)	10000	12000	18000	15000	
Type	vertical	horizontal	vertical	vertical	
Shell					
Materials			SUS-27	SUS-27	J.I.S. designation
Inner diam. (mm)	297	297	420	420	
Outer diam. (mm)	300	300	423	423	
Total height (mm)	705+(100)	805	804+(100)	638+[175]+(100)	[ ]: coil support height,
Center duct	with	without	with	with	
Inner diam. (mm)	158	—	158	158	( ): leg height
Outer diam. (mm)	160	—	160	160	
Water jacket	with	with	without	without	
Outer diam. (mm)	350	322	—	—	
Height (mm)	555	500	—	—	
Heat insulator					
Material	R.W.	R.W.	R.W.	R.W.	R.W.: rockwool
Coils					
Materials	Al coated steel	Al coated steel	SUS-28, SUS-32 M-5, S-TEN-1 Al coated S-TEN-1	SUS-32 NTK-30A	
Inner diam. (mm)	17	17	14	14	
Outer diam. (mm)	22	22	18	18	
Inner coil					
Coil diam. (mm)	200	139	200	200	
Pitch (mm)	30	30	30	30	
Number of turns	15	23	25	20	
2nd coil					
Coil diam. (mm)	260	198	260	260	
Pitch (mm)	30	30	30	30	
Number of turns	16	23	25	20	
3rd coil					
Coil diam. (mm)	—	257	320	320	
Pitch (mm)	—	30	30	30	
Number of turns		24	25	20	
4th coils					
Coil diam. (mm)	—	—	380	380	
Pitch (mm)	—	—	30	30	
Number of turns	—	—	25	20	
Total coil length (m)	23.5	45.8	94.3	75.5	
Total outer surface area of coils (m²)	1.62	3.17	5.33	4.27	
Water jacket surface area (m²)	0.52	0.50	0	0	
Total heating area F_o (m²)	2.14	3.67	5.33	4.27	
Overall coefficient of heat transmission K_{lm} (kcal/m²h°C)	—	—	19.5	19.5	
Electric generators (kVA)	20	20	45/65	45/65	

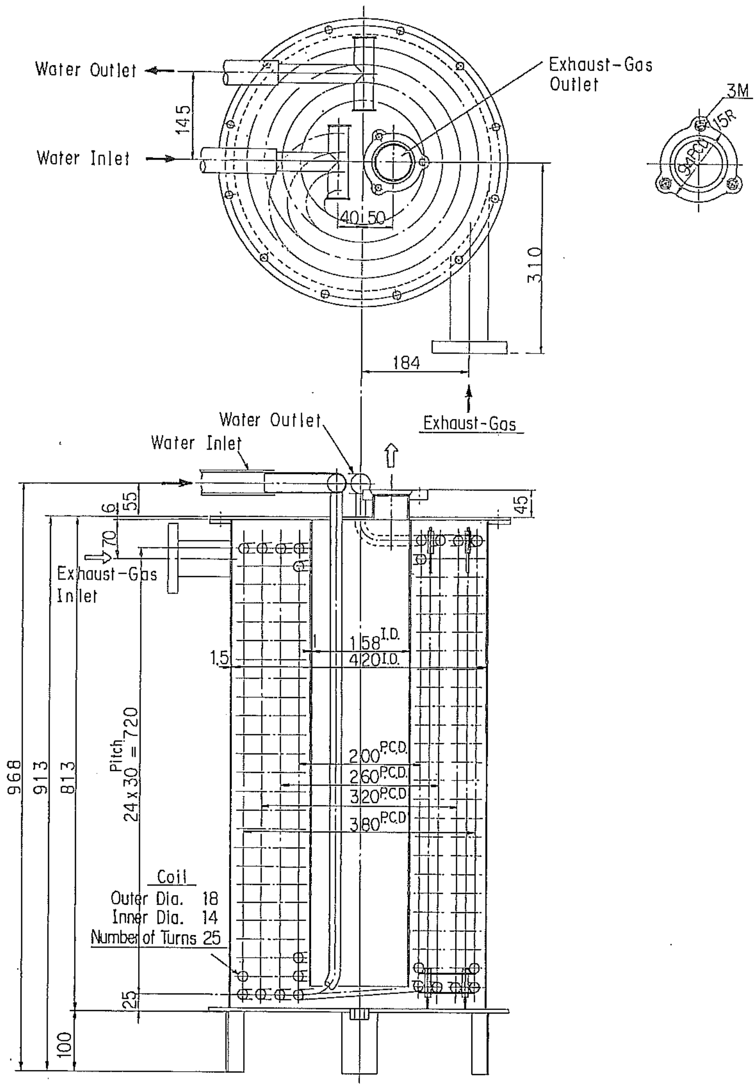

Fig. 29. Shell-and-coil type heat exchanger used during JARE-7/15.

of coils made of stainless steel such as SUS-304L, -316, -316L and others as shown in Fig. 32. Several materials shown in Table 8 were tested as coil materials and among these materials NIK30-A was the best, followed by M-5, although these were not perfect materials.

Some systems for avoiding acid corrosion of coils were tried at Syowa Station. The first was a binary system for avoiding direct cooling of the exhaust gas by cold water. First, the exhaust-gas heat exchanger warmed hot water, and then the hot water heated the cold water through a vertical shell-and-tube type water-to-water heat exchanger as shown in Fig. 55. The binary system as shown in Figs. 16, 18 and 21 were very effective for preventing corrosion of coils.

The second method was to neutralize the sulfuric acid with a weak alkaline

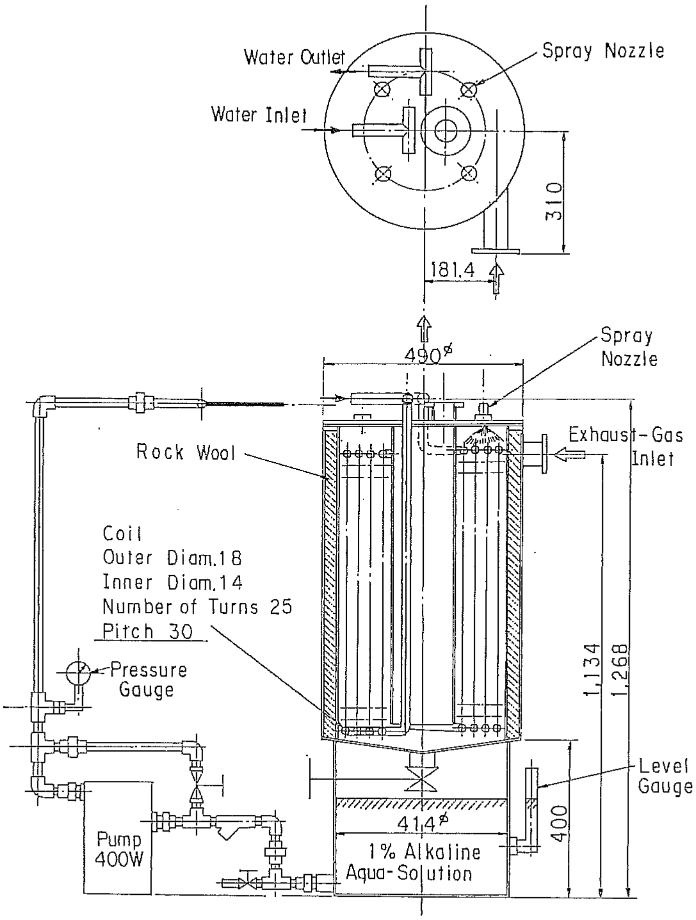

Fig. 30. Shell-and-coil type exhaust-gas heat exchanger provided with alkaline aqua-solution spraying nozzles (JARE-16/18).

aqua solution, such as 1% of CaOH. Fig. 30 shows the system, which was prepared for JARE-16/18 (1974/78). The exhaust-gas heat exchanger was mounted on an alkaline solution reservoir tank. The solution was pumped up by a small pump, and the pressurized solution was injected through four low-pressure spray nozzles installed on the top cover plate. By spraying the solution over the four coils in the shell from time to time, acid corrosion could be prevented somewhat, and at the same time, the soot adhering to the coil surface could be dissolved into the solution.

(b) Decrease of heat transfer with time due to soot accumulation on coil surface

As is well known, another important problem relating to exhaust-gas heat exchangers used for diesel engines is the decrease of heat transfer with time cause by increased heat resistance due to an adhering soot layer on exchanger heating surfaces.

Figs. 33 and 34 show the results of observation in the JARE-7 engine room

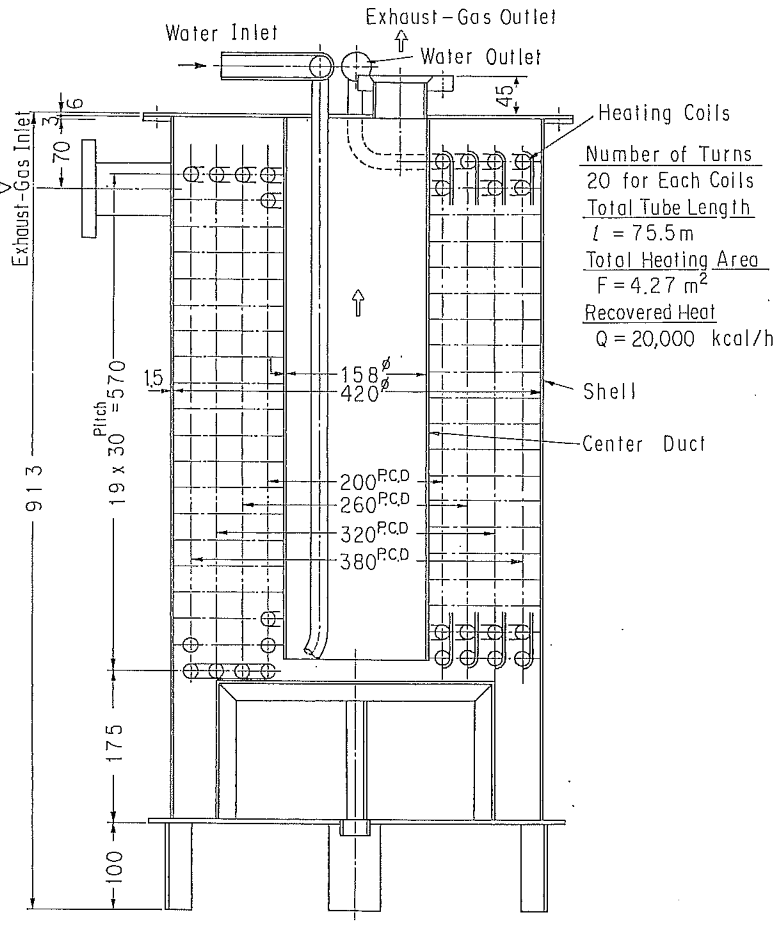

Fig. 31. Shell-and-coil type exhaust-gas heat exchanger with a bottom chamber for collecting soot (JARE-16/18).

Fig. 32. Severe acid corrosion of stainless-steel coils by exhaust gas of diesel engine (Materials, SUS-316 and SUS-304).

Table 8. Materials used for heating coils of exhaust-gas heat exchangers.

JIS Standard	C	Si	P	Mn	S	Ni	Cr	Mo	Sb	Cu
SUS-304L (SUS-28)	<0.02	<1.00	<0.04	<2.00	<0.03	9–13	18–20	—	—	—
SUS-316 (SUS-32)	<0.08	<1.00	<0.04	<2.00	<0.03	10–14	16–18	2–3	—	—
SUS-316L (SUS-33)	<0.03	<1.00	<0.04	<2.00	<0.03	12–15	16–18	2–3	—	—
NIK 30-A (NAS-305)	<0.06	<1.00	<0.03	<2.00	<0.02	28–31	19–21	2–3	—	2.75–3.75
M-5	<0.06					15–17	17–19	4.5–6	—	—
S-TEN-1	0.09	0.35	0.019	0.42	0.022	—	—	—	0.098	0.34

Note: 1) SUS-304L: Severe acid corrosion was observed.
2) SUS-316, SUS-316L: Some acid corrosion was observed, but less than SUS-304L.
3) NIK 30-A: called Carpenter-20; can resist acid corrosion.
4) M-5: can resist acid corrosion.
5) S-TEN-1: was developed by Shin Nihon Seitetsu Co., Ltd.; does not contain Ni and Cr but can resist acid corrosion. Alumered S-TEN-1 was used as coil material, but internal surface of coil cannot be alumered.

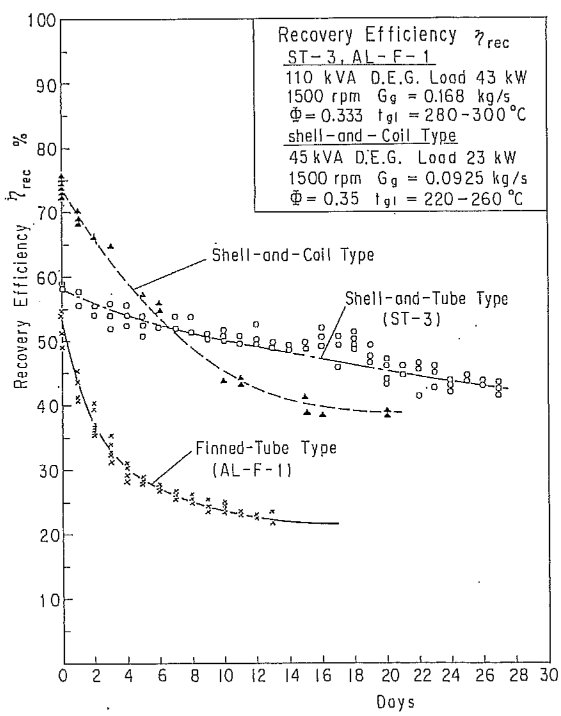

Fig. 33. Decreasing recovery efficiency η_{rec} of exhaust-gas heat exchanger due to soot layer adhering to heating surfaces.

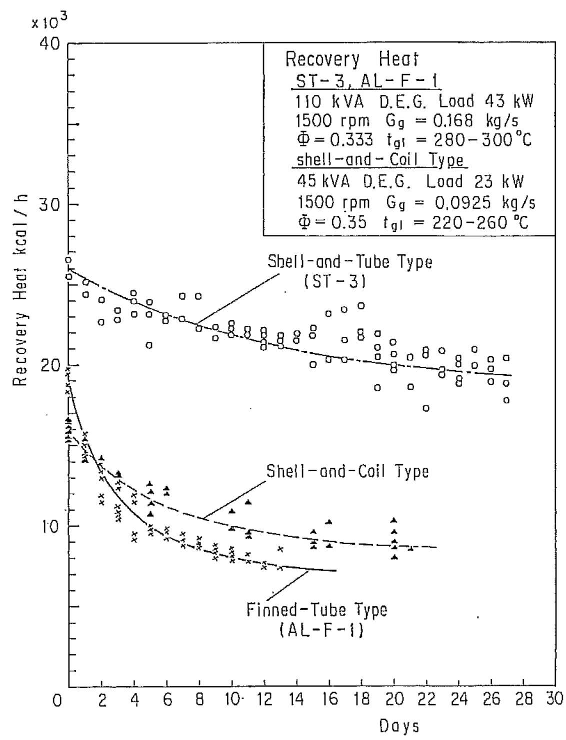

Fig. 34. Decreasing recovered heat Q_R by exhaust-gas heat exchangers due to soot layer adhering to heating surfaces.

(JARE-14, 1973) and in the JARE-9 engine room (JARE-19, 1978) by TAKEUCHI, one of the authors. In these experiments, the inlet gas temperature t_{g1} of the heat exchanger and the outlet temperature t_{g2} were recorded electrically over a period of 20 to 30 days.

The heat Q_R recovered by an exhaust-gas heat exchanger is expressed by eq. (17) and is nearly proportional to the temperature difference $(t_{g1}-t_{g2})$ and to the gas flow rate G_g. The recovery efficiency η_{rec} defined by eq. (26) can also be calculated. As shown in Fig. 33, the recovery efficiency of the shell-and-coil type is about 73% at the start but decreases to 40% after three weeks because of soot adhering to coil surfaces, so that it is necessary to clean off the soot from time to time.

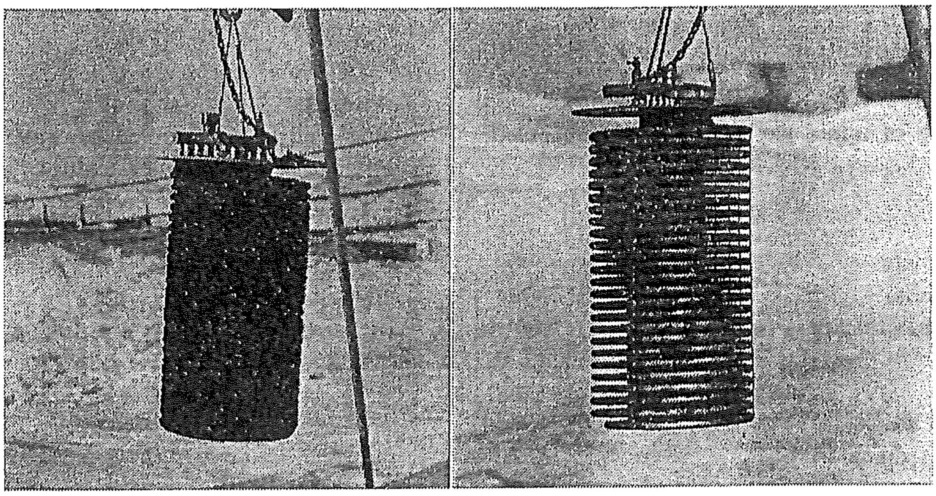

Fig. 35. Cleaning of soot adhering to heating coil of exhaust-gas heat exchanger by blizzard (TAKEUCHI, JARE-14). Left: before cleaning, right: after cleaning in blizzard.

As shown in Fig. 35, TAKEUCHI succeeded in removing the soot adhering to the coil by hanging it in a storm wind. This is a very interesting method, but care must be taken to cause all of the water remaining in the coil to be drained off completely by pressurized air, because frozen water in the coil will rupture the coil tube.

In the shell-and-coil type heat exchanger, the engine exhaust gas flows tangentially into the shell at its top part and flows down around the coils to its bottom, then rising through the center duct connected to a chimney by a flexible pipe. Hence, the heat exchanger itself can be considered as a cyclone separator, and the separated soot is accumulated at the bottom of the shell and chokes the gas flow to the center duct. Fig. 31 shows an improved type having a bottom space to avoid the choking of gas flow by the accumulated soot.

Table 9. Vertical shell-and-tube type exhaust-gas heat exchangers for JARE.

Items	JARE-19 (1977/79)	JARE-20 (1978/80)	JARE-21 (1979/81)
Type	ST-1	ST-2	ST-3
Capacity (kcal/h)	15000/25000	15000/25000	25000
Shell			
Material	SUS-304	SUS-304	SUS-304
Inner diam. (mm)	500	500	540
Outer diam. (mm)	504	504	546
Height (mm)			
Upper gas chamber	120	120	150
Shell	800	800	800
Lower gas chamber	150 (SUS-304)	150 (SUS-304)	120 (FC-25)
Legs	100 (SUS-304)	100 (SUS-304)	115 (FC-25)
Total	1179	1179	1179
Heat insulator			
Material	rock wool	without	without
Cooling of upper gas chamber	uncooled	uncooled	cooled by water outer diam. of water jacket 616 mm (205 mm from top)
Tube plate			
Material	SUS-304	SUS-304	SUS-304
Diam.×thickness (mm)	500×6t	500×6t	upper 538×10t lower 630×10t
Tubes			
Material	SUS-304	SUS-304TB	SUS-316TB-A
Inner diam. (mm)	23	23	21.4 22.4
Outer diam. (mm)	25.4	25.4	25.4 25.4
Tube length (mm)	800	800	800 800
Number of tubes	112	112	112 112
Outer surface area (m^2)	7.15	7.15	7.15 7.15
Inner surface area (m^2)	6.47	6.47	6.02 6.31
Working fluid			
Shell side	water	water	water
Area A_w (m^2)	0.0698	0.0698	0.0861 0.0861
Tube side	gas	gas	gas
Area A_g (m^2)	0.0233	0.0233	0.02014 0.02207
Velocity (m/s) (V_g=0.164 m^3/s)	7.04	7.04	8.15 7.44
Overall coefficient of heat transmission K_{lm} (kcal/m^2h°C)	28.2	28.2	35.1
Recovery efficiency η_{rec}	0.57	0.74	0.72
Temperature efficiency Φ_g (gas side)	0.90	0.91	0.86

It should be noted that the shell-and-coil type heat exchanger is very effective as an exhaust noise supressor, so that an engine silencer is unnecessary. The heat loss from an exhaust manifold and exhaust pipe conducting the exhaust gas from the engine to the heat exchanger is very great, so that they should be insulated thermally, and the length of the exhaust pipe conducting the gas to the heat exchanger should be kept as short as possible.

6.2. Vertical shell-and-tube type exhaust-gas heat exchangers (Table 9)

For simplifying the keeping clear of soot, the shell-and-coil type has been changed to a vertical shell-and-tube type as shown in Fig. 36 in which the exhaust gas flows down and turns up through the inside of heating tubes, and the

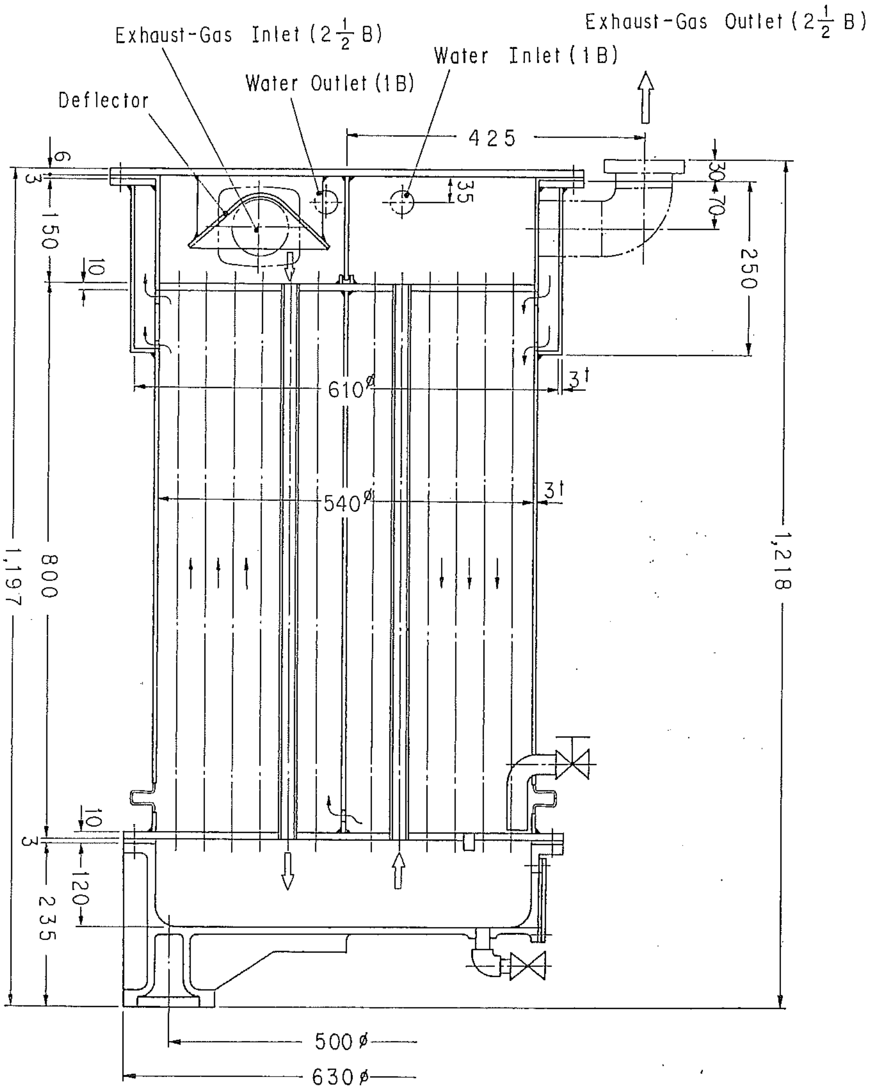

Fig. 36. Shell-and-tube type exhaust-gas heat exchanger ST-3 prepared for JARE-21 (1979/81).

water flows through the shell side (JARE-19, 1977/79). The heating capacity was increased to 21000–25000 kcal/h as shown in Fig. 34 and Table A-5 in Appendix and was sufficient for recovering the waste heat of the 110-kVA diesel-electric generator in the JARE-9 engine room. The prototype ST-1 (JARE-19) and ST-2 (JARE-20, 1978/1980) were made entirely of stainless steel SUS-304 pipes and sheets welded together. Inlet gas chambers were not cooled by water, but the shell under the top tube plate was contacted by water directly, so that excess thermal stress and failure occurred on the shell surfaces just below the top tube plate as shown in Fig. 37.

For removing the excess thermal stress on the shell surfaces, the upper inlet gas chamber was also water-cooled in an improved type ST-3 (JARE-21, 1979/81) as shown in Figs. 36 and 38. In this type, the shell is made of SUS-304 stainless-steel sheets, and the heating tubes are made of SUS-316L or TB-A and are 800 mm in length. The bottom box was cast from FC-25 and had an opening with a cover plate for occasionally scraping out the accumulated soot. In the

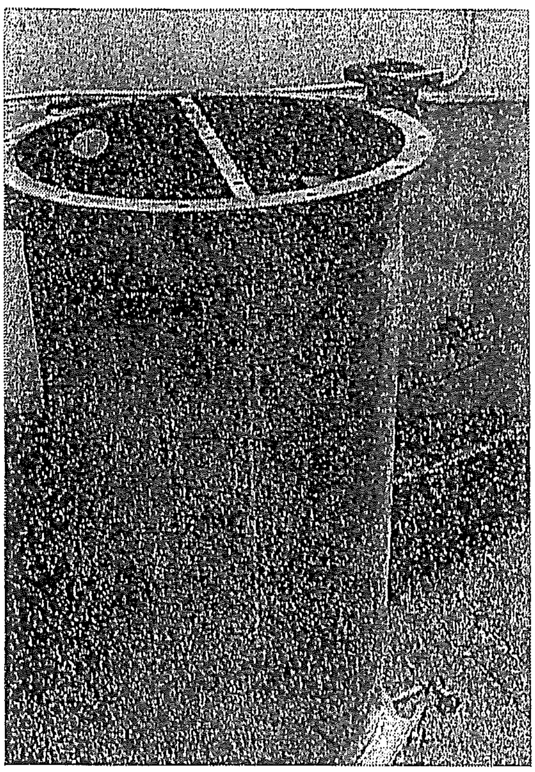

Fig. 37. Repaired thermal crack occurring on the boundary of water jacket and uncooled shell surface heated by inlet high temperature exhaust-gas jet in ST-2 prepared for JARE-20 (1978/80).

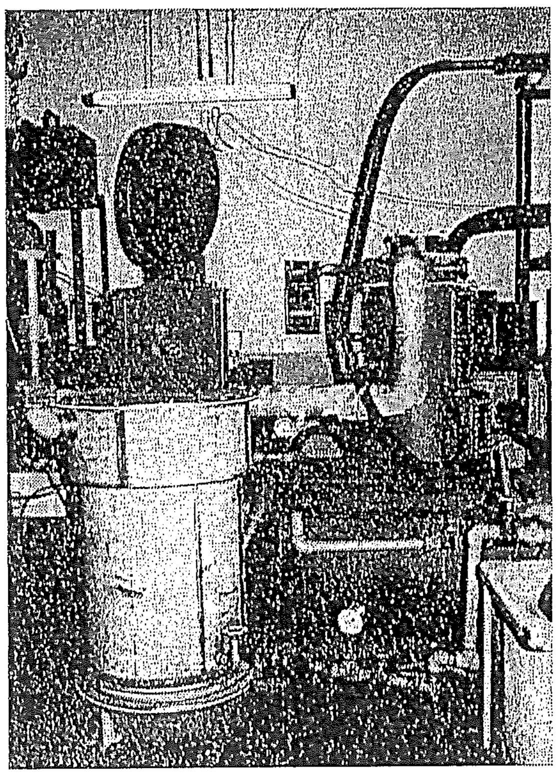

Fig. 38. ST-3 shell-and-tube type exhaust-gas heat exchanger being tested in Engine Laboratory of Nihon University, Tokyo (6 October 1979).

ST-3 type, the soot adhering on the inner surfaces of vertical heating tubes can be scraped off easily without touching any part of the water system by removing only the top cover plate. The theoretical and experimental analyses of the ST-3 type are shown in Appendix 2. The fouling effect of soot is less than that in the shell-and-coil type as shown in Figs. 33 and 34.

6.3. Vertical fin-tube type exhaust-gas heat exchangers

A vertical fin-tube type heat exchanger AL-F-1 as shown in Table 10 and Fig. 39 was developed by the authors for JARE-19. It is composed of an aluminum cylinder with 36 longitudinal axial fins, a water-cooled shell, and a center tube made of SUS-304. The engine exhaust gas flows down through the axial fins to the bottom and turns up through the center tube connected to a chimney.

Cold water conducted to an inlet at the bottom of the heat exchanger rises up through an annular passage formed between the center tube and the inner surface of the finned cylinder to its outlet and is conducted again to the bottom of outer water jacket of shell by a pipe.

The estimated fin efficiency is about 98.6%, so that the total fin area can be considered as the same as a direct heating area.

The maximum heating capacity of the AL-F-1 is about 18000 kcal/h at the start as shown in Fig. 34, but decreases to about 7000 kcal/h after two weeks due to soot fouling. Generally, the heating capacity of an exhaust-gas heat exchanger Q_R is represented by

$$Q_R = K_{am}F(t_{gm} - t_{wm}) = K_{lm}F\Delta t_{lm} \text{ kcal/h}, \tag{34}$$

where

t_{gm}: mean gas temperature, °C,
t_{wm}: mean water temperature, °C,
Δt_{lm}: logarithmic mean temperature difference, °C,

$$\Delta t_{lm} = (\Delta t_1 - \Delta t_2)/\ln(\Delta t_1/\Delta t_2) \quad \text{(counterflow)}, \tag{35}$$
$$\Delta t_1 = t_{g1} - t_{w2}, \qquad \Delta t_2 = t_{g2} - t_{w1},$$

t_{g1}: inlet gas temperature, °C, t_{g2}: outlet gas temperature, °C,
t_{w1}: inlet water temperature, °C, t_{w2}: outlet water temperature, °C,
K_{am}: overall coefficient of heat transmission for arithmetic mean temperature difference, kcal/m²h°C,
K_{lm}: overall coefficient of heat transmission for logarithmic mean temperature difference, kcal/m²h°C,
F: a standard heating area, here, the area of the gas side being taken as F, m².

Table 10. Vertical fin-tube type exhaust-gas heat exchangers prepared for JARE.

Items	AL-F-1 JARE-19 (1977/79)	AL-F-2 JARE-21 (1979/81)	AL-F-3 JARE-22 (1980/82)
Type	built-up	integrally cast	built-up
Capacity Q_R (kcal/h)	18000	18000	24000
Total heating area F_o (m^2)	5.704	5.971	6.754
Overall coefficient of heat transmission			
K_{lm} (kcal/m^{2}h°C)	25.6	26.3	28.5
$K_{lm}F_o$ (kcal/h°C)	146	157	192
Shell			
Material	SUS-304	AC4A-T6	SUS-304
Inner diam.×thickness	400×2t	418×8t	444.4×6.4t
Outer diam.×thickness	500×2t	554×10t	556×3t
Vertical length	794	800	800
Heating surface area (gas side) F_s (m^2)	0.998	3.050	1.116
Coefficient of heat transfer (kcal/m^{2}h°C)			
Water side α_{w1}	135	112	223
Gas side α_g	10.0	11.6	28.8
Overall coefficient of heat transmission			
K_s (kcal/m^{2}h°C)	9.31	10.5	25.5
K_sF_s (kcal/h°C)	9.29	32.0	29.5
Fin tube			
Material	AC4A-T6	AC4A-T6	AC4A-T6
Tip radius of fin (mm)	199	209	222
Hub radius of fin (mm)	125	129	125
Thickness of fin at tip (mm)	8	10	7
Thickness of fin at hub (mm)	13	10	13
Height of fin (mm)	74	80	97
Number of fins	36	36	36
Vertical length of fin (mm)	764	800	800
Vertical length of tube (mm)	794	800	800
Total fin area F_f (m^2)	4.071	2.304	5.587
Fin efficiency η_f	0.986	0.993	0.93
Hub area of fin F_h (m^2)	0.242	0.361	0.254
Tip area of fin F_t (m^2)	0.220	0.762	0.202
Equivalent directly heating area F_{fd} (m^2)	4.473	2.695	5.638
Coefficient of heat transfer (kcal/m^{2}h°C)			
Water side α_{w2}	215	189	308
Gas side α_g	10.0	11.6	28.8
Overall coefficient of heat transmission			
K_f (kcal/m^{2}h°C)	9.65	10.9	26.3
K_fF_{fd} (kcal/h°C)	42.8	29.4	148.3

Items	AL-F-1 JARE-19 (1977/79)	AL-F-2 JARE-21 (1979/81)	AL-F-3 JARE-22 (1980/82)
Center tube			
Material	SUS-304	A-6063	(AC4A-T6)
Inner diam.×thickness (mm)	93.6×4t	90×5t	230
Outer diam. (mm)	101.6	100	
Vertical length (mm)	794	800	763
Heating surface area F_T (m^2)	0.233	0.226	center partition
Coefficient of heat transfer (kcal/m^2 h°C)			plate SUS-304
Water side α_{w2}	215	189	(169B×760H×3t)
Gas side α_{gT}	37.5	53.7	
Overall coefficient of heat transmission			
K_T (kcal/m^2h°C)	31.9	41.8	
K_TF_T (kcal/h°C)	7.44	9.45	

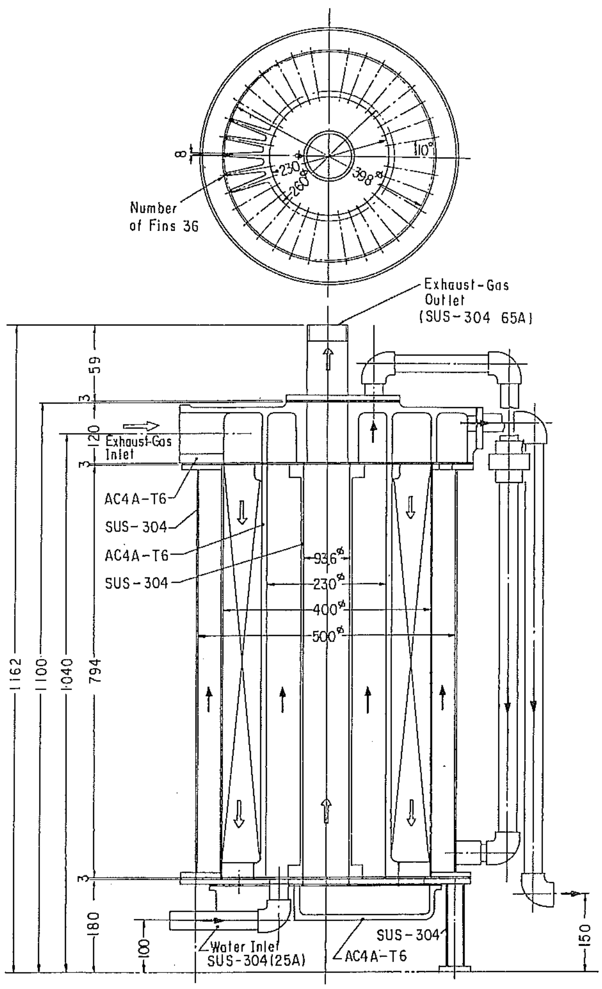

Fig. 39. Fin-tube type exhaust-gas heat exchanger AL-F-1 prepared for JARE-19 (1977/79).

The overall coefficient of heat transmission through a wall depends mainly on the heat transfer coefficient of the gas side, α_g, because the heat transfer coefficient of the water side, α_w, is much greater than α_g. Hence, for increasing K_{lm} or K_{am}, the heat transfer coefficient of the gas side, α_g should be increased, and the latter is proportional to the gas velocity. Accordingly, for increasing Q_R with the same

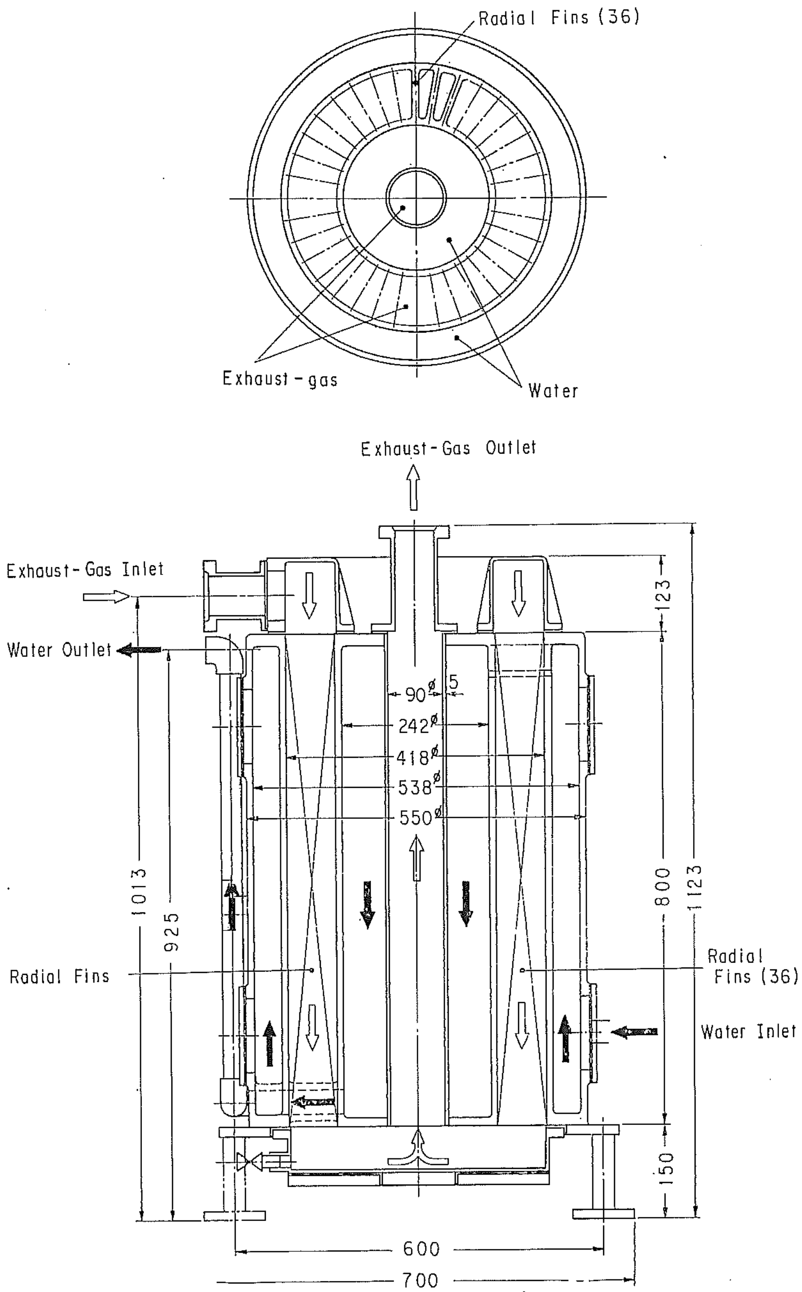

Fig. 40. Integrally cast fin-tube type exhaust-gas heat exchanger AL-F-2 prepared for JARE-21 (1979/81).

heating surface area F, the gas velocity in the heat exchanger should be kept as high as possible.

The merits of the fin-tube type exhaust-gas heat exchanger are as follows:

(a) Aluminum fins are kept at high temperature and protected from acid corrosion, whereby durability will be improved compared with that of shell-and-coil or shell-and-tube types.

(b) The soot adhering to its heating surfaces can be scraped off easily by removing the top cover only.

(c) The cost will be lower than that of the ST-3 type because of the simplicity of manufacturing.

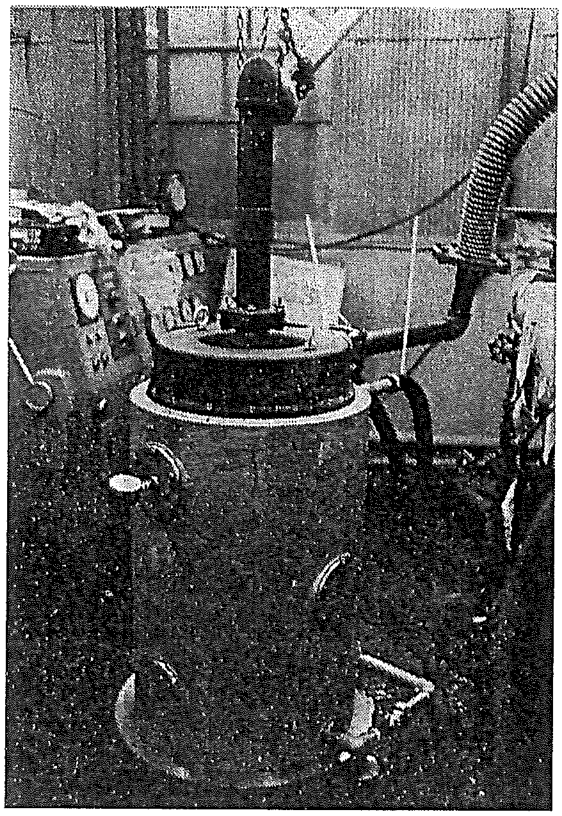

Fig. 41. Integrally cast aluminum fin-tube type exhaust-gas heat exchanger AL-F-2 prepared for JARE-21 (1979/81).

In the AL-F-1, the water piping system had to be removed to remove soot. To overcome this defect, the AL-F-2 type as shown in Figs. 40 and 41 was manufactured for JARE-21. It is composed of three parts, *i.e.*, an uncooled top cover with gas inlet and outlet made of FC-25, an integrally cast aluminum center body with axial fins and a water jacket, and a bottom cover made of SUS-304. However, the AL-F-2 has two demerits, one of which is the difficulty of integrally casting the body. The other is that rapid cooling of the heated center body must be

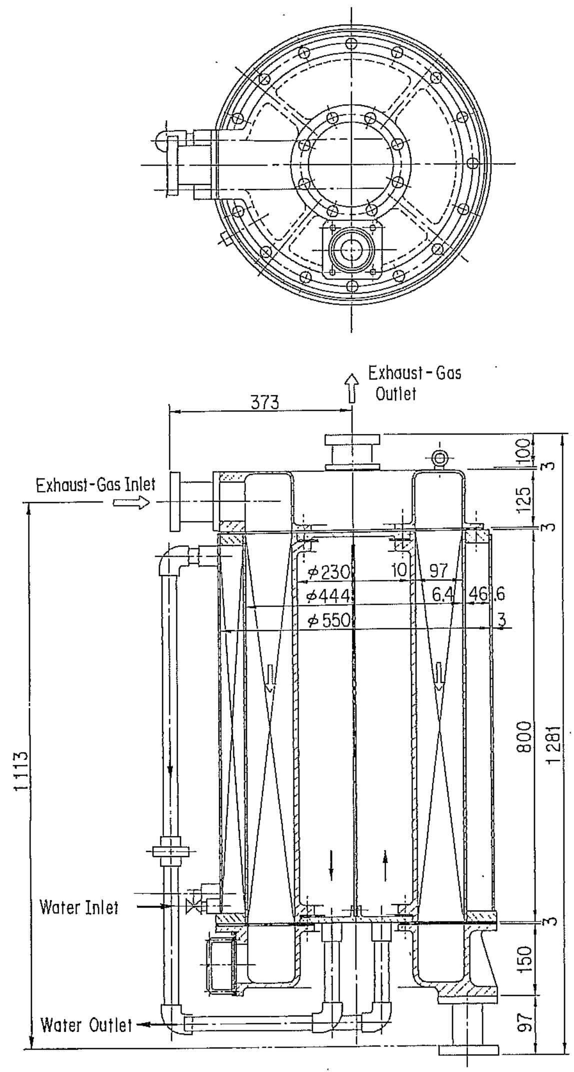

Fig. 42. Fin-tube type exhaust-gas heat exchanger AL-F-3 prepared for JARE-22 (1980/82).

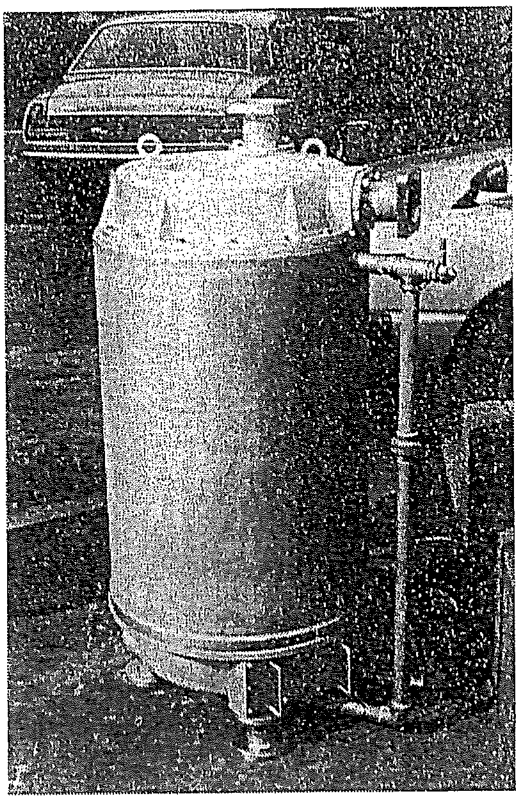

Fig. 43. Fin-tube type exhaust-gas heat exchanger AL-F-3 prepared for JARE-22.

strictly avoided to prevent mechanical failure due to excessive thermal stress.

For JARE-22 (1980/82), AL-F-3 was prepared. This is an improved type of AL-F-1 as shown in Figs. 42 and 43. The exhaust-gas velocity in this new type is 9.66 m/s and K_{lm} was increased to 28.5 kcal/m^{2}h°C compared with 4.28 m/s and 25.6 kcal/m^{2}h°C in the AL-F-1. Moreover, soot scraping can be done without touching the water system.

7. Experimental Analysis of Exhaust-Gas Heat Exchangers

As described above, the authors developed three kinds of heat exchangers for recovering the waste heat of diesel engines. These heat exchangers were tested in the Engine Laboratory of Nihon University, Tokyo, before they were shipped to Antarctica. A turbocharged high-speed diesel engine, Isuzu-640T, coupled to an electric eddy-current dynamometer was used as the exhaust-gas source. The engine is of the same type as that used for the 65-kVA diesel-electric power generator at Syowa Station (see Table 3). The heat balance of this engine is shown in Fig. 27 and Table 6c.

The experimental equipment is shown in Fig. 44. The exhaust gas of the diesel engine is introduced into an exhaust-gas heat exchanger being tested, and the outlet gas is sucked in by a Nash pump and delivered into the atmosphere through a chimney. As a heating load, a bathtub filled with water was used, and

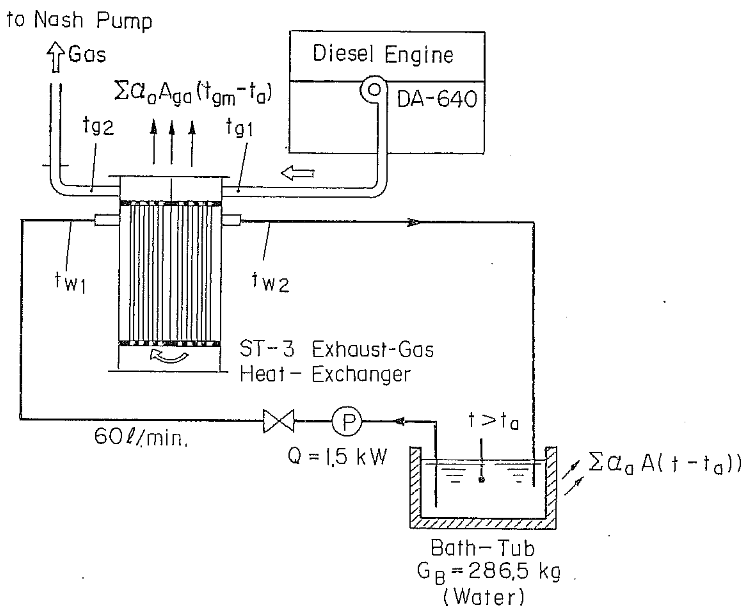

Fig. 44. Experimental equipment for testing exhaust-gas heat exchangers in Engine Laboratory of Nihon University, Tokyo.

a water pump recirculated the hot water between the water side of the heat exchanger and the bathtub.

As an example, the test on a shell-and-tube type ST-3 heat exchanger will be described below.

G_g: weight flow of exhaust gas, kg/h,
c_{pgm}: mean specific heat at constant pressure of exhaust gas, kcal/kg°C,
t_{gm}: mean gas temperature $t_{gm}=(t_{g1}+t_{g2})/2$, °C,
t_a: atmospheric air temperature, °C,
A_{ga}: cooling surface area of heat exchanger, contacting exhaust gas at one side and atmosphere at the other side, m^2,
α_g: heat transfer coefficient of gas side, kcal/m^{2}h°C,
α_w: heat transfer coefficient of water side, kcal/m^{2}h°C,
α_a: heat transfer coefficient of air side due to natural convection, kcal/m^{2}h°C,
R_g: thermal resistance of gas side boundary layer, m^{2}h°C/kcal,
R_c: thermal resistance of soot layer, m^{2}h°C/kcal,
R_w: thermal resistance of water side boundary layer, m^{2}h°C/kcal,
R_m: thermal resistance of metal wall, m^{2}h°C/kcal,
λ_c: thermal conductivity of soot, kcal/mh°C,
λ_m: thermal conductivity of metal wall, kcal/mh°C,
F_i: internal surface area of tubes, m^2,
F_o: external surface area of tubes, m^2,
l: length of one tube, m,
z: number of tubes in one path area,
d_i: internal diameter of tube, m,
d_o: external diameter of tube, m,
D_s: inner diameter of shell, m,
δ_c: thickeness of soot layer, m,
δ_m: thickness of metal wall, m,
c_M: specific heat of heated material, kcal/kg°C,
G_M: weight of heated material, kg,
G_B: total weight of water contained in bathtub, kg,
Φ_g: temperature efficiency of gas side,
c_w: specific heat of water, $c_w=1.0$ kcal/kg°C,
t: mean water temperature in bathtub, °C,
τ: time, h,
$\eta_{\rm rec}$: recovery efficiency.

After starting the engine, measurements were made every 5 minutes until the mean water temperature of the bathtub became substantially constant. The following four methods for estimating the heating capacity of the heat exchanger Q_R, overall coefficient of heat transmission K_{lm} or K_{am}, recovery efficiency η_{rec}, and temperature efficiency Φ_g can be recommended.

(a) Q_{R1} obtained by measurement of exhaust-gas temperatures t_{g1} and t_{g2}

The heat transferred from hot exhaust gas to water in the heat exchanger can be calculated by

$$Q_{R1}=G_g c_{pgm}(t_{g1}-t_{g2})-\sum\alpha_a A_{ga}(t_{gm}-t_a) \text{ kcal/h}, \tag{36}$$

$$G_g=G_a+G_f \text{ kg/h}, \tag{37}$$

where G_g denotes the total exhaust gas containing steam, and c_{pgm} is its mean specific heat at constant pressure for mean gas temperature t_{gm}. The first term of eq. (36) represents the apparent total enthalpy drop, and the second term indicates the heat loss from the hot parts of the shell, contacting hot gas on its inside and room air on its outer side, respectively. The cooling surface area A_{ga} and the heat transfer coefficient α_a should be estimated theoretically.

As an example, for ST-3 (Fig. 36) $t_{gm}=207°\text{C}$, $t_a=19°\text{C}$,
for top cover plate $A_{ga}=0.229 \text{ m}^2$, $\alpha_a=5.75 \text{ kcal/m}^2\text{h}°\text{C}$,

$$\alpha_a A_{ga}=1.32 \text{ kcal/h}°\text{C}$$

for bottom box $A_{ga}=0.229 \text{ m}^2$, $\alpha_a=2.00 \text{ kcal/m}^2\text{h}°\text{C}$, $\alpha_a A_{ga}=0.46 \text{ kcal/h}°\text{C}$,

$$\sum\alpha_a A_{ga}(t_{gm}-t_a)=1.78(207-19)=335 \text{ kcal/h}.$$

The results of experiments are shown in Table A-5 in Appendix. The heating capacity Q_{R1} obtained by this method will be most accurate, because the temperature difference $(t_{g1}-t_{g2})$ is very great, although the weight flow rate of the air and fuel should be measured experimentally.

In the case of counter flow, the overall coefficient of heat transmission K_{lm} and K_{am} can be obtained from eqs. (34) and (35) by putting

$$F=F_i=2z(\pi d_i l)=2(56)[\pi(0.0214)(0.800)]=6.02 \text{ m}^2,$$

$$\begin{aligned}1/K_{lm}&=\sum R=R_g+R_c+R_m+R_w\\&=(1/\alpha_g)(F_i/F_c)+(\delta_c/\lambda_c)+(\delta_m/\lambda_m)+(1/\alpha_w)(F_i/F_o) \text{ m}^2\text{h}°\text{C/kcal},\end{aligned} \tag{38}$$

where F_c is the internal surface area of the soot layer. At the start, $F_c=F_i$ and $\delta_c=0$, because the internal surface of the tubes is clean.

The arithmetic temperature difference Δt_{am} is represented by

$$\Delta t_{am}=t_{gm}-t_{am}=(t_{g1}+t_{g2})/2-(t_{w1}+t_{w2})/2=(\Delta t_1+\Delta t_2)/2 \;°\text{C}. \tag{39}$$